Plane-wave propagation and radiation patterns in attenuative TI media

Yaping Zhu and Ilya Tsvankin
Center for Wave Phenomena, Dept. of Geophysics, Colorado School of Mines, Golden, CO 80401

ABSTRACT
Directionally-dependent attenuation coefficient in transversely isotropic (TI) formations can have a significant influence on the amplitudes of reflected waves and distort the results of AVO (amplitude variation with offset) analysis. Here, we develop a consistent analytic treatment of plane-wave properties and point-source radiation for TI media with attenuation anisotropy.
The anisotropic quality factor can be described by matrix elements Q_{ij} defined as the ratios of the real and the imaginary parts of the corresponding stiffness coefficients. For the special "isotropic" case of $Q_{ij} = \text{const}$ the attenuation coefficient is independent of angle, even if the symmetry of the velocity anisotropy is lower than TI. To characterize TI attenuation, we follow the idea of Thomsen notation for velocity anisotropy and replace the components Q_{ij} by two reference isotropic quantities and three dimensionless anisotropic parameters ϵ_Q, δ_Q, and γ_Q. The parameters ϵ_Q and γ_Q quantify the difference between the horizontal and vertical attenuation coefficients of P- and SH-waves (respectively), while δ_Q is defined through the second derivative of the P-wave attenuation coefficient in the symmetry direction. Although the definitions of ϵ_Q, δ_Q, and γ_Q are similar to those for the corresponding Thomsen parameters, the expression for δ_Q reflects the coupling between the attenuation and velocity anisotropy.
Assuming weak attenuation as well as weak velocity and attenuation anisotropy allows us to obtain simple linearized attenuation coefficients expressed through the Thomsen-style parameters. The attenuation coefficients for both P- and SV-waves have the same form as the corresponding approximate phase-velocity functions, but the effective attenuation-anisotropy parameter for SV-waves depends on the velocity parameter σ in addition to ϵ_Q and δ_Q. The linearized approximations not only provide analytic insight into the behavior of the attenuation coefficients, they also remain accurate for the practically important range of small and moderate anisotropic coefficients, in particular for near-vertical and near-horizontal propagation directions.
We also employ the stationary-phase method to derive the far-field Green's function for arbitrarily anisotropic media with TI attenuation. The influence of the attenuation on the radiation patterns is absorbed by an exponential term that depends on the "group" attenuation coefficient along the raypath. The relationship between the group and phase (plane-wave) attenuation coefficients involves just the group and phase angles and can be used to estimate the Thomsen-style parameters from wide-angle attenuation measurements.

Key words: attenuation, attenuation anisotropy, transverse isotropy, radiation pattern, point source, seismic amplitude

1 INTRODUCTION

Attenuation is a process that dissipates the energy and alters both the amplitude and the frequency content of elastic waves. The influence of attenuation on the amplitudes of reflected waves may cause errors in AVO (amplitude variation with offset) analysis. For example, Blangy (1994) speculates that some unexplained pitfalls in AVO interpretation may be attributed to attenuation-related phenomena. Reflection and transmission coefficients in layered attenuative media are discussed in Ursin and Stovas (2002) and in transversely isotropic (TI) media by Carcione (1997). More significant distortions of the AVO response, however, may be caused by the attenuation along the raypath of the reflected wave, in particular if the attenuation coefficient is angle-dependent.

For azimuthally anisotropic formations that contain systems of small-scale aligned fractures, both velocity and attenuation vary with azimuth. The azimuthal variation of the attenuation coefficient can be used to estimate the orientation and some physical properties of the fractures (Rathore et al, 1995; Lynn et al, 1999; Chichinina et al., 2004).

Physical-modeling experiments (Hosten et al., 1987; Arts and Rasolofosaon, 1992) show that attenuation in anisotropic rocks can be directionally dependent, and the attenuation anisotropy is sometimes more significant than the velocity anisotropy (Hosten et al., 1987; Arts and Rasolofosaon, 1992). Similar results are obtained by Carcione (2000) using numerical modeling for North Sea Kimmeridge shales. Prasad and Nur (2003) observed P-wave attenuation anisotropy for reservoir rocks (such as fluvial sandstones and dolomites) by measuring the attenuation coefficient in two orthogonal directions. Their experiments indicate that the attenuation anisotropy can be related to the texture of sedimentary rocks.

Although the physical mechanism of intrinsic attenuation is not yet clearly understood, a number of parameters have been introduced to quantify attenuation-related amplitude decay (e.g., Johnston and Toksöz, 1981). The most common choices are the quality factor Q and the magnitude of the imaginary part of the complex wavenumber, which is usually called the attenuation coefficient. A comprehensive discussion of wave propagation in anisotropic attenuative media is given by Carcione (2001). His treatment, however, is generally based on the stiffness coefficients c_{ij}, and the results are not expressed in a form amenable to data-processing applications. As demonstrated below, analysis of the influence of anisotropic attenuation on seismic signatures can be facilitated by introducing dimensionless anisotropic parameters responsible for the angle-dependent quality factor.

The terminology in this paper is designed to draw a clear distinction between velocity and attenuation anisotropy. To ensure consistency with existing literature on anisotropic elastic media, terms such as *anisotropic media* or *TI (transversely isotropic) media* refer to the velocity anisotropy. When discussing attenuative media, we explicitly specify the character of the attenuation. For example, the term *TI medium with isotropic attenuation* means that the model is transversely isotropic with respect to the velocity function but the attenuation is isotropic (i.e., independent of direction).

The first part of this paper is devoted to plane-wave signatures in TI media with both isotropic and TI attenuation. The discussion is limited to *homogeneous* wave propagation which means that the real and imaginary part of the wave vector are parallel to each other. After defining the quality factor Q through the ratios of the real and imaginary parts of the stiffness coefficients, we introduce Thomsen-style parameters that describe the angle-dependent Q for TI attenuation. The advantages of the new notation are demonstrated by analyzing the attenuation coefficient as a function of phase angle. To gain insight into the behavior of the attenuation coefficients for P- and SV-waves, we simplify the exact equations under the assumptions that the attenuation and velocity anisotropy, as well as the attenuation itself, are weak. The accuracy of the approximate attenuation coefficients is verified by several numerical tests for representative TI models.

By employing the formalism of Tsvankin and Chesnokov (1990) and Tsvankin (2001, Chapter 2), we derive a closed-form expression for the radiation patterns in homogeneous TI media with TI attenuation. To express the results in terms of the attenuation along the raypath (i.e., the group attenuation), we find a simple relationship between the group and phase attenuation and illustrate it with numerical simulation of SH-wave propagation from a point source.

2 TI MEDIA WITH ISOTROPIC ATTENUATION

2.1 Definition of the Q factor

The quality factor Q can be related to several other parameters used in attenuation measurements, such as the attenuation coefficient, logarithmic decrement of amplitude, and complex modulus (Johnston and Toksöz, 1981). All those parameters, however, were originally designed for isotropic attenuation and need to be generalized for anisotropic materials.

To develop a consistent description of Q for both isotropic and anisotropic attenuation, we follow Carcione (2001, p. 58) in defining Q as twice the time-averaged strain-energy density divided by the time-averaged dissipated-energy density. In terms of the complex stiffness coefficients, Q is given by

$$Q_{ij} \equiv \frac{c_{ij}}{c_{ij}^I}, \tag{1}$$

where c_{ij} and c_{ij}^I are the real and the imaginary parts, respectively, of the stiffness coefficient $\tilde{c}_{ij} = c_{ij} + ic_{ij}^I$. Note that there is no summation over i and j in equation (1).

The analysis below is restricted to transversely isotropic media with either isotropic or TI attenuation. The symmetry axis is assumed to be vertical, but since all results are derived for a homogeneous medium, they can be readily adapted to TI models with any symmetry-axis orientation.

Since Q is expressed as the ratio of the real and imaginary parts of the complex stiffness coefficients, the matrix formed by the Q components inherits the structure of the stiffness matrix. For the case of VTI media with VTI attenuation, the $\mathbf{Q}$ matrix has the form

$$\mathbf{Q} = \begin{bmatrix} Q_{11} & Q_{12} & Q_{13} & 0 & 0 & 0 \\ Q_{12} & Q_{11} & Q_{13} & 0 & 0 & 0 \\ Q_{13} & Q_{13} & Q_{33} & 0 & 0 & 0 \\ 0 & 0 & 0 & Q_{55} & 0 & 0 \\ 0 & 0 & 0 & 0 & Q_{55} & 0 \\ 0 & 0 & 0 & 0 & 0 & Q_{66} \end{bmatrix}, \qquad (2)$$

where $Q_{12} = Q_{11}\dfrac{c_{11} - 2c_{66}}{c_{11} - 2c_{66}\,Q_{11}/Q_{66}}$.

When both the velocity and attenuation are isotropic, the $\mathbf{Q}$ matrix includes only two independent parameters, Q_{33} and Q_{55}:

$$\mathbf{Q} = \begin{bmatrix} Q_{33} & Q_{13} & Q_{13} & 0 & 0 & 0 \\ Q_{13} & Q_{33} & Q_{13} & 0 & 0 & 0 \\ Q_{13} & Q_{13} & Q_{33} & 0 & 0 & 0 \\ 0 & 0 & 0 & Q_{55} & 0 & 0 \\ 0 & 0 & 0 & 0 & Q_{55} & 0 \\ 0 & 0 & 0 & 0 & 0 & Q_{55} \end{bmatrix}. \qquad (3)$$

The component Q_{33} controls the P-wave attenuation, while Q_{55} is responsible for the SV-wave attenuation (see below). The component $Q_{13} = Q_{12}$ can be obtained from Q_{33} and Q_{55} as

$$Q_{13} = Q_{33}\frac{c_{33} - 2c_{55}}{c_{33} - 2c_{55}\,Q_{33}/Q_{55}}. \qquad (4)$$

According to the attenuation measurements in sandstones by Gautam et al. (2003), the Q-factor for P-waves may be either larger or smaller than that for SV-waves, depending on the mobility of fluids in the rock. The "crossover" frequency, for which $Q_{33} = Q_{55}$, corresponds to the special case when all components of the $\mathbf{Q}$ matrix are identical:

$$Q_{ij} \equiv Q. \qquad (5)$$

As discussed below, if $\mathbf{Q}$ is described by equation (5), the attenuation for both P- and S-waves is isotropic (independent of direction), even for arbitrarily anisotropic media.

The $\mathbf{Q}$ matrix can be obtained by calculating the so-called eigenstiffnesses from the stiffness matrix and applying relaxation functions to the eigenstiffnesses in order to characterize the anisotropic attenuation (Helbig, 1994; Carcione, 2001). The complex stiffness coefficients $\tilde{c}_{ij}$ and the matrix $\mathbf{Q}$ are then obtained from the eigenstiffnesses. For TI media, these operations are described in detail by Carcione (2001, Chapter 4).

The discussion here is based on the assumption of a frequency-independent Q, which is often valid in the seismic frequency band. In a more rigorous description of attenuation, the complex stiffness components and the factor Q vary with frequency, as does the velocity. Treatment of velocity dispersion, however, is outside the scope of this paper.

2.2 Christoffel equation for attenuative media

The displacement of a harmonic plane wave can be written as

$$\tilde{\mathbf{u}} = \tilde{\mathbf{U}} \exp\left[i(\omega t - \tilde{\mathbf{k}}\mathbf{x})\right], \qquad (6)$$

where $\tilde{\mathbf{U}}$ denotes the polarization vector, t is the time, and ω is the angular frequency. The vector $\tilde{\mathbf{k}}$ denotes the complex wave vector, $\tilde{\mathbf{k}} = \mathbf{k} - i\mathbf{k}^I$; the imaginary part, $\mathbf{k}^I$, can be called the attenuation vector. By substituting the plane wave (6) into the wave equation, we obtain the Christoffel equation for attenuative media:

$$\left[\tilde{G}_{ik} - \rho\tilde{V}^2\delta_{ik}\right]\tilde{U}_k = 0. \qquad (7)$$

Here, $\tilde{G}_{ik} = \tilde{c}_{ijkl}n_j n_l$ is the Christoffel matrix that depends on the complex stiffnesses $\tilde{c}_{ijkl}$ and the unit vector $\mathbf{n}$ in the phase direction, ρ is the density, δ_{ik} is Kronecker's symbolic δ, and $\tilde{V} = \dfrac{\omega}{\tilde{k}}$ is the complex phase velocity. The real part V of the phase velocity is given by (Carcione, 2001)

$$V = \left[\mathrm{Re}\left(\frac{1}{\tilde{V}}\right)\right]^{-1} = \frac{\omega}{k}. \qquad (8)$$

2.3 SH-wave attenuation for media with isotropic Q

For waves propagating in the $[x_1, x_3]$-plane of VTI media, the Christoffel equation (7) splits into an equation for the SH-wave polarized in the x_2-direction and two coupled equations for the in-plane polarized P- and SV-waves. The equation for the wave vector of the SH-wave has the same form as that in non-attenuative media:

$$\tilde{c}_{66}\tilde{k}_1^2 + \tilde{c}_{55}\tilde{k}_3^2 - \rho\omega^2 = 0. \qquad (9)$$

As shown in Appendix A2, for a medium with isotropic Q ($Q = Q_{55} = Q_{66}$), the imaginary part of equation (9) reduces to

$$\mathcal{K}_2 \equiv \frac{k^2 - (k^I)^2}{Q} - 2kk^I = 0, \qquad (10)$$

where k and k^I are the real and imaginary parts (respectively) of the wave vector. Note that the assumption of isotropic Q for SH-waves does not involve the

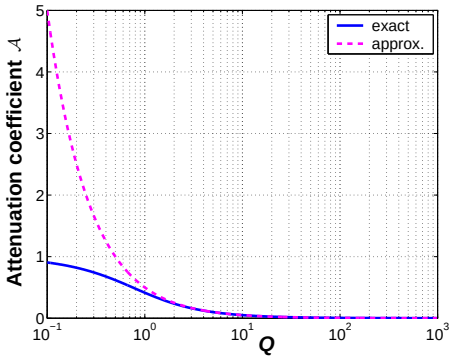

Figure 1. Normalized attenuation coefficient $\mathcal{A}$ for SH-waves as a function of the Q factor for a medium with $Q_{55} = Q_{66} = Q$. The solid line is the exact $\mathcal{A}$ from equation (10); the dashed line is the weak-attenuation approximation (13).

condition $Q_{33} = Q_{55}$. Solving for k^I, we find [also see equation (2.122) in Carcione (2001)]

$$k^I = k(\sqrt{1+Q^2} - Q)\,. \tag{11}$$

It is convenient to introduce the normalized attenuation coefficient $\mathcal{A}$ that defines the rate of amplitude decay per wavelength:

$$\mathcal{A} \equiv \frac{k^I}{k}\,. \tag{12}$$

Equation (11) shows that $\mathcal{A}$ for SH-waves in media with isotropic Q is independent of the phase angle. When the attenuation is weak (i.e., $\frac{1}{Q} \ll 1$), equation (11) yields

$$\mathcal{A} \equiv \frac{k^I}{k} \approx \frac{1}{2Q}\,. \tag{13}$$

The weak-attenuation approximation (13) is close to the exact attenuation coefficient $\mathcal{A}$ for the practically important range $Q > 10$ (Figure 1). Equation (13) breaks down only for strongly attenuative media with $Q < 2$.

The real part of the Christoffel equation (9) has the form (Appendix A)

$$(c_{66}n_1^2 + c_{55}n_3^2)\mathcal{K}_1 - \rho\omega^2 = 0\,, \tag{14}$$

where

$$\mathcal{K}_1 \equiv k^2 - (k^I)^2 + \frac{2kk^I}{Q}\,. \tag{15}$$

Expressing k^I from equation (11), we find $\mathcal{K}_1$ as a function of k:

$$\mathcal{K}_1 = k^2\frac{2(\sqrt{1+Q^2} - Q)(1+Q^2)}{Q}\,. \tag{16}$$

Substituting equation (16) into equation (14) yields the phase velocity of the SH-wave:

$$V_{SH}(\theta) = V_{SH}^{\text{elast}}(\theta)\,\xi_Q\,, \tag{17}$$

where V_{SH}^{elast} is the phase velocity in the reference purely elastic medium expressed through the phase angle θ ($n_1 = \sin\theta$, $n_3 = \cos\theta$),

$$V_{SH}^{\text{elast}}(\theta) = \sqrt{\frac{c_{66}\sin^2\theta + c_{55}\cos^2\theta}{\rho}}\,, \tag{18}$$

and

$$\xi_Q = \sqrt{\frac{2(\sqrt{1+Q^2} - Q)(1+Q^2)}{Q}}\,. \tag{19}$$

In the limit of weak attenuation, $\mathcal{K}_1$ becomes

$$\mathcal{K}_1 \approx k^2(1 + \frac{1}{Q^2})\,, \tag{20}$$

and the phase velocity simplifies to

$$V_{SH}(\theta) = V_{SH}^{\text{elast}}(\theta)\left(1 + \frac{1}{2Q^2}\right)\,. \tag{21}$$

For a realistic range of Q values, the influence of the attenuation on the real part of the wavenumber and, therefore, on the phase velocity, is of the second order and can be ignored. Even for strongly attenuative media with $Q = 5$, the contribution of the term $\frac{1}{2Q^2}$ in equation (21) is limited to 2% of the velocity V_{SH}.

2.4 P-SV wave attenuation for media with isotropic Q

If the **Q** matrix has the form (3) with $Q_{33} \neq Q_{55}$, the attenuation of P- and SV-waves can still be directionally dependent (section 5). The P- and SV-wave phase velocities in a medium of this type are given by

$$V_P(\theta) = V_P^{\text{elast}}(\theta)\left[1 + \text{O}\left(\frac{1}{Q_{33}^2}\right)\right]\,, \tag{22}$$

and

$$V_{SV}(\theta) = V_{SV}^{\text{elast}}(\theta)\left[1 + \text{O}\left(\frac{1}{Q_{55}^2}\right)\right]\,, \tag{23}$$

where $V_P^{\text{elast}}(\theta)$ and $V_{SV}^{\text{elast}}(\theta)$ are the phase velocities in the reference purely elastic model. As discussed above for SH-waves, the influence of the attenuation on the phase velocities can be ignored even for relatively small values of Q_{33} and Q_{55}.

If we further assume that $Q_{33} = Q_{55}$, which corresponds to the special case of isotropic $Q \equiv Q_{ij}$, the properties of P- and SV-waves become similar to those of SH-waves (Appendix B2). The P- and SV-wave attenuation coefficients are described by equations (10) and (13), and the contribution of the attenuation to the phase velocities is given by the factor ξ_Q from equation (19).

3 TI MEDIA WITH TI ATTENUATION

Since the real and imaginary parts of the wave vector are coupled in the Christoffel equation, the directional dependence of the attenuation is influenced by the velocity anisotropy of the material. The physical reasons for the attenuation and velocity anisotropy in TI media may also be similar. For example, preferential orientation of clay platelets in shales may be responsible not just for the intrinsic velocity anisotropy (Sayers, 1994), but also for the velocity anisotropy. Therefore, it is reasonable to assume that the symmetry of the attenuation in TI media is the same as that of phase velocity. Furthermore, in the discussion below the symmetry axes of the attenuation coefficient and velocity function are taken to be parallel to each other.

3.1 SH-wave attenuation for media with TI Q

For the general TI form of the matrix $\mathbf{Q}$ in equation (2), the Christoffel equation yields the following relationship between the real and imaginary wavenumbers (Appendix A1):

$$k^2 - (k^I)^2 - 2Q_{55}\alpha k k^I = 0\,, \tag{24}$$

where

$$\alpha \equiv \frac{(1+2\gamma)\sin^2\theta + \cos^2\theta}{(1+2\gamma)\dfrac{Q_{55}}{Q_{66}}\sin^2\theta + \cos^2\theta}\,, \tag{25}$$

where γ is Thomsen's velocity-anisotropy parameter for SH-waves. Solving equation (A5) for k^I, we find the SH-wave attenuation coefficient:

$$\mathcal{A} \equiv \frac{k^I}{k} = \sqrt{1+(Q_{55}\,\alpha)^2} - Q_{55}\,\alpha\,. \tag{26}$$

In the weak-attenuation limit, equation (26) reduces to

$$\mathcal{A} = \frac{1}{2Q_{55}\,\alpha}\,. \tag{27}$$

Equation (27) shows that Q_{55} is multiplied with the parameter α to form the effective quality factor for the SH-wave, $Q_{55}^{\text{eff}} = Q_{55}\,\alpha$. At vertical incidence ($\theta = 0°$), $\alpha = 1$ and $\mathcal{A} = \dfrac{1}{2Q_{55}}$. In the horizontal direction ($\theta = 90°$), $\alpha = \dfrac{Q_{66}}{Q_{55}}$ and $\mathcal{A} = \dfrac{1}{2Q_{66}}$. For intermediate propagation directions, α reflects the coupling between the SH-wave velocity-anisotropy parameter γ and the ratio of Q_{55} and Q_{66}. The contribution of the ratio Q_{55}/Q_{66} to equation (25) is used below to define an attenuation-anisotropy parameter analogous to γ.

3.2 P-SV wave attenuation for media with TI Q

Because of the coupling between P- and SV-waves, the equations governing their velocity and attenuation are more complicated than those for SH-waves. While the complex wavenumbers for P- and SV-waves can be evaluated numerically from equations (B3)–(B4), the imaginary wavenumber k^I is difficult to obtain in closed form. Therefore, here we employ approximate solutions to study the dependence of the attenuation coefficients of P- and SV-waves on the medium parameters.

If both the attenuation anisotropy and the attenuation itself are weak, the coefficient $\mathcal{A}$ for both P- and SV-waves is given by (see Appendix C1)

$$\mathcal{A} = \frac{1}{2Q_{33}}(1+\mathcal{H})\,, \tag{28}$$

where $\mathcal{H} = \dfrac{\mathcal{H}_u}{\mathcal{H}_d}$,

$$\begin{aligned}\mathcal{H}_u = &\left(c_{11}n_1^2\frac{Q_{33}-Q_{11}}{Q_{11}} + c_{55}n_3^2\frac{Q_{33}-Q_{55}}{Q_{55}}\right)\\ &(c_{55}n_1^2 + c_{33}n_3^2 - \rho V^2)\\ &+c_{55}n_1^2\frac{Q_{33}-Q_{55}}{Q_{55}}(c_{11}n_1^2 + c_{55}n_3^2 - \rho V^2)\\ &-2\left(c_{13}\frac{Q_{33}-Q_{13}}{Q_{13}} + c_{55}\frac{Q_{33}-Q_{55}}{Q_{55}}\right)(c_{13}+c_{55})n_1^2n_3^2\,,\end{aligned} \tag{29}$$

and

$$\mathcal{H}_d = \rho V^2[(c_{55}+c_{11})n_1^2 + (c_{33}+c_{55})n_3^2 - 2\rho V^2]\,. \tag{30}$$

V is the phase velocity of either the P- or SV-wave, depending on which attenuation coefficient is desired.

The parameter $\mathcal{H}$ is responsible for the contribution of the attenuation anisotropy. For the P-wave, $\mathcal{H} = 0$ results in $\mathcal{A}_P = \dfrac{1}{2Q_{33}}$, and the P-wave attenuation becomes isotropic. For the SV-wave, isotropic attenuation implies that $\mathcal{H} = \dfrac{Q_{33}-Q_{55}}{Q_{55}}$, which yields $\mathcal{A}_{SV} = \dfrac{1}{2Q_{55}}$.

Note that for P-waves at vertical incidence ($\theta = 0°$), $\mathcal{H} = 0$, and $\mathcal{A}_P = \dfrac{1}{2Q_{33}}$. In the horizontal direction ($\theta = 90°$), $\mathcal{H} = \dfrac{Q_{33}-Q_{11}}{Q_{11}}$ and $\mathcal{A}_P = \dfrac{1}{2Q_{11}}$. Hence, $\mathcal{H} = \dfrac{Q_{33}-Q_{11}}{Q_{11}}$ gives the fractional difference between the P-wave attenuation coefficients in the horizontal and the vertical directions and can be used to characterize the P-wave attenuation anisotropy (see the next section).

For SV-waves the value $\mathcal{H} = \dfrac{Q_{33}-Q_{55}}{Q_{55}}$ is the same for both the vertical and the horizontal directions, and the coefficient $\mathcal{A}_{SV} = \dfrac{1}{2Q_{55}}$ at both directions.

The high accuracy of the approximate solutions for $\mathcal{A}$ is confirmed by the example in Figure 2. The model is elliptical for the velocity anisotropy since $\epsilon = \delta$, but the shape of the attenuation coefficients is strongly nonel-

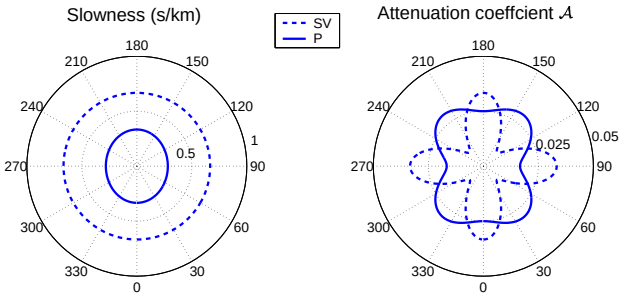

Figure 2. Slownesses (left) and the attenuation coefficients $\mathcal{A}$ (right) of P-waves (solid curves) and SV-waves (dashed) as functions of the phase angle. The coefficients $\mathcal{A}$ were computed from approximation (28) and substituted into equation (B3) to obtain the slownesses. The model parameters are V_{P0}=3 km/s, V_{S0}=1.5 km/s, $\epsilon = \delta = 0.2$, $Q_{11} = 30$, $Q_{33} = 20$, $Q_{13} = 15$, and $Q_{55} = 15$. (The Q components correspond to the attenuation anisotropy parameters $\epsilon_Q = -0.33$ and $\delta_Q = 0.98$ defined in the next section.)

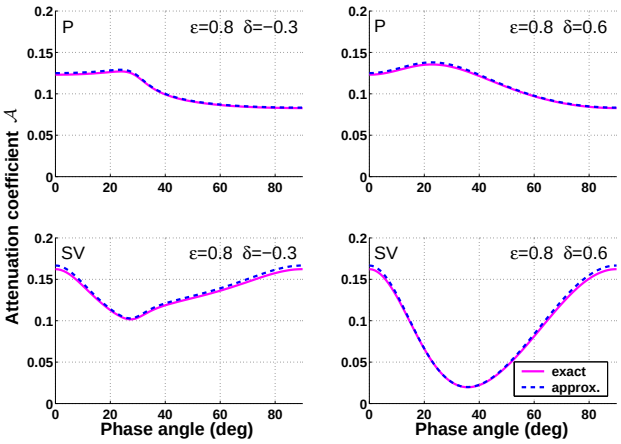

Figure 3. Normalized attenuation coefficients for P-waves (top row) and SV-waves (bottom row) computed for two different pairs of the parameters ϵ and δ marked on the plot. The solid curves are the exact solutions from equations (B3) and (B4), the dashed curves mark approximation (28). The other model parameters are V_{P0}=3 km/s, V_{S0}=1.5 km/s, $Q_{11} = 4$, $Q_{33} = 3$, $Q_{13} = 2$, and $Q_{55} = 3$.

liptical. The attenuation coefficients on the right plot in Figure 2 were computed from equations (28)–(30). The evaluated $\mathcal{A}$ were then substituted into equation (B3) to estimate the real part of the wavenumber and calculate the slownesses of P- and SV-waves shown on the left. The approximate attenuation coefficients and slownesses practically coincide with the exact solutions obtained by jointly solving equations (B3) and (B4). Since the error of the approximations is negligible, the exact solutions are not plotted in Figure 2. This test also demonstrates that the phase velocities are virtually unchanged in the presence of moderate attenuation.

The approximate solution (28) for $\mathcal{A}$ remains accurate even for models with much more significant attenuation and larger values of the velocity-anisotropy parameters ϵ and δ (Figure 3). Note that in both the vertical ($\theta = 0°$) and horizontal ($\theta = 90°$) directions the attenuation is independent of ϵ or δ. However, the shape of the attenuation curves at intermediate angles varies with both ϵ or δ, especially when the velocity anisotropy is strong.

4 THOMSEN-STYLE NOTATION FOR TI ATTENUATION

The description of seismic signatures in the presence of velocity anisotropy can be substantially simplified by using Thomsen (1986) notation. The advantages of Thomsen parameters in the analysis of seismic velocities and amplitudes for TI media are discussed in detail by Tsvankin (2001).

Here, we extend the idea of Thomsen notation to the directionally dependent attenuation coefficient in TI media. The matrix $\mathbf{Q}$ for models with TI attenuation contains five independent elements, which can be replaced by two reference (isotropic) parameters and three dimensionless coefficients (ϵ_Q, δ_Q, and γ_Q) responsible for the attenuation anisotropy. Since we operate with the attenuation coefficient, which is inversely proportional to the quality factor, we define the Thomsen-style parameters through quantities $\frac{1}{Q_{ij}}$. To maintain close similarity with Thomsen notation for velocity anisotropy, we choose the P- and SV-wave attenuation coefficients in the symmetry direction ($\frac{1}{Q_{33}}$ and $\frac{1}{Q_{55}}$) as the reference values. (The coefficient $\frac{1}{Q_{55}}$ is also responsible for the SV-wave attenuation in the horizontal plane.)

4.1 SH-wave parameter γ_Q

We define the attenuation anisotropy parameter γ_Q for SH-waves as the fractional difference between the attenuation coefficients in the horizontal and vertical directions [see equation (27)]:

$$\gamma_Q \equiv \frac{1/Q_{66} - 1/Q_{55}}{1/Q_{55}} = \frac{Q_{55} - Q_{66}}{Q_{66}}. \qquad (31)$$

This definition is analogous to that of the Thomsen parameter $\gamma = (c_{66} - c_{55})/(2c_{55})$, which is close to the fractional difference between the horizontal and vertical velocities of the SH-wave. The parameter γ_Q controls the magnitude of the SH-wave attenuation anisotropy; for isotropic Q, $\gamma_Q = 0$.

Substituting γ_Q into equation (25) for the parame-

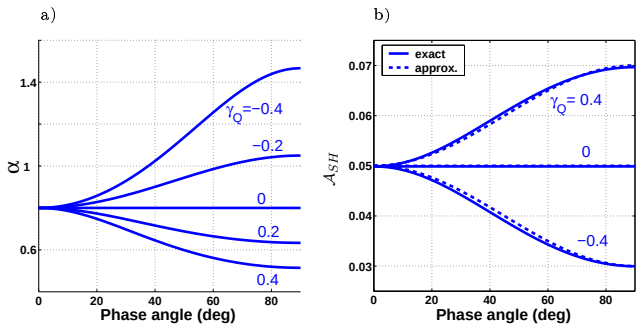

Figure 4. Factor α (a) and the attenuation coefficient $\mathcal{A}_{SH}$ (b) for the SH-wave in a TI medium with $\gamma = 0.1$, $Q_{55} = 10$, and γ_Q varying from -0.4 to 0.4. The exact $\mathcal{A}_{SH}$ is computed from equation (26), and the approximate $\mathcal{A}_{SH}$ from equation (34).

ter α yields

$$\alpha = \frac{(1+2\gamma)\sin^2\theta + \cos^2\theta}{(1+2\gamma)(1+\gamma_Q)\sin^2\theta + \cos^2\theta}\,. \tag{32}$$

When both γ and γ_Q are small ($|\gamma| \ll 1$, $|\gamma_Q| \ll 1$), α can be linearized in these parameters:

$$\alpha = 1 - \gamma_Q \sin^2\theta\,. \tag{33}$$

The attenuation coefficient from equation (27) then becomes

$$\mathcal{A}_{SH} = \frac{1}{2Q_{55}}(1 + \gamma_Q \sin^2\theta)\,. \tag{34}$$

Equation (34) has the same form as the SH-wave phase velocity linearized in the parameter γ (Thomsen, 1986).

It is clear from equation (34) that γ_Q determines the rate and sign of the variation of $\mathcal{A}_{SH}(\theta)$ away from the vertical (symmetry) direction. When $\gamma_Q > 0$, the factor α decreases with the phase angle θ, which causes an increase in the attenuation coefficient (Figure 4). In contrast, for negative γ_Q the coefficient $\mathcal{A}_{SH}(\theta)$ decreases with angle. If the magnitude of the velocity anisotropy is small (i.e., $|\gamma| \ll 1$), approximation (34) gives an accurate estimate of the attenuation coefficient even for relatively large absolute values of γ_Q reaching 0.4 (Figure 4b).

4.2 P-SV wave parameters ϵ_Q and δ_Q

The attenuation-anisotropy parameter ϵ_Q can be defined by analogy with the Thomsen parameter ϵ:

$$\epsilon_Q = \frac{1/Q_{11} - 1/Q_{33}}{1/Q_{33}} = \frac{Q_{33} - Q_{11}}{Q_{11}}\,, \tag{35}$$

ϵ_Q is equal to the fractional difference between the P-wave attenuation coefficients in the horizontal and vertical directions.

To complete the description of TI attenuation, we need to introduce a parameter similar to the Thomsen's δ that involves the quality-factor component Q_{13}. It seems that we can simply adapt the definition of δ by replacing the stiffnesses c_{ij} with $1/Q_{ij}$:

$$\hat{\delta}_Q \equiv \frac{(1/Q_{13} + 1/Q_{55})^2 - (1/Q_{33} - 1/Q_{55})^2}{2/Q_{13}(1/Q_{33} - 1/Q_{55})}\,. \tag{36}$$

The parameter $\hat{\delta}_Q$ from equation (36), however, is not physically meaningful. For example, when the attenuation is isotropic and $Q_{33} = Q_{55}$ (Gautam et al., 2003), the anisotropic parameters are supposed to vanish. Instead, $\hat{\delta}_Q$ for isotropic Q goes to infinity.

As discussed by Tsvankin [2001, see equation (1.49)], the parameter δ proved to be extremely useful in describing the signatures of reflected P-waves in VTI media because it determines the second derivative of the P-wave phase-velocity function in the vertical (symmetry) direction (the first derivative goes to zero). Therefore, although the expression for δ in terms of the stiffness coefficients cannot be directly adapted to attenuative media, a physically meaningful definition of δ_Q can be obtained from the second derivative of the P-wave attenuation coefficient $\mathcal{A}_P$ at $\theta = 0$:

$$\left.\frac{d^2\mathcal{A}_P}{d\theta^2}\right|_{\theta=0} = 2\mathcal{A}_P|_{\theta=0}\,\delta_Q\,. \tag{37}$$

In other words, the parameter δ_Q controls the curvature of the coefficient $\mathcal{A}_P$ in the vertical direction.

Assuming that both the attenuation and the attenuation anisotropy are weak, we find the following explicit expression for δ_Q (Appendix C):

$$\delta_Q \equiv \frac{\dfrac{Q_{33}-Q_{55}}{Q_{55}}c_{55}\dfrac{(c_{13}+c_{33})^2}{(c_{33}-c_{55})} + 2\dfrac{Q_{33}-Q_{13}}{Q_{13}}c_{13}(c_{13}+c_{55})}{c_{33}(c_{33}-c_{55})}\,. \tag{38}$$

The role of δ_Q in describing the P-wave attenuation anisotropy is similar to that of δ in the P-wave phase-velocity equation (Thomsen, 1986; Tsvankin, 2001). Since the first derivative of $\mathcal{A}_P$ for $\theta = 0$ is equal to zero, δ_Q is responsible for the angular variation of the P-wave attenuation coefficient near the vertical direction.

In the special case of a purely isotropic (i.e., angle-independent) velocity function, δ_Q reduces to a weighted summation of the fractional differences $(Q_{33}-Q_{55})/Q_{55}$ and $(Q_{33}-Q_{13})/Q_{13}$:

$$\delta_Q = \frac{Q_{33}-Q_{55}}{Q_{55}}\frac{4\mu}{\lambda+2\mu} + \frac{Q_{33}-Q_{13}}{Q_{13}}\frac{2\lambda}{\lambda+2\mu}\,, \tag{39}$$

where λ and μ are the Lame parameters.

Unless attenuation is uncommonly strong, the phase velocities of P-and SV-waves are close to those in the purely elastic medium and do not depend on the attenuation parameters ϵ_Q and δ_Q. Equation (38) for

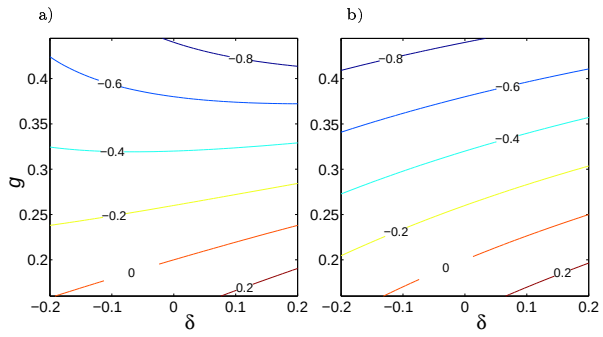

Figure 5. Contour plot of the parameter δ_Q as a function of δ and $g \equiv V_{S0}^2/V_{P0}^2$ computed from (a) equation (41), and (b) equation (42). The other parameters are $Q_{33} = 4$, $Q_{55} = 8$, and $Q_{13} = 3$. The range of g values corresponds to $1.5 < V_{P0}/V_{S0} < 2.5$.

the parameter δ_Q, however, indicates that the attenuation anisotropy is influenced by the velocity anisotropy. If we approximate c_{13} as $c_{13} = c_{33}(1+\delta) - 2c_{55}$, which can be done for small $|\delta|$ (Tsvankin, 2001, p. 20), and denote

$$g \equiv \frac{V_{S0}^2}{V_{P0}^2} = \frac{c_{55}}{c_{33}}, \tag{40}$$

δ_Q can be rewritten as

$$\delta_Q = \frac{Q_{33}-Q_{55}}{Q_{55}} g \frac{(2+\delta-2g)^2}{(1-g)^2} + \frac{Q_{33}-Q_{13}}{Q_{13}} \frac{2(1+\delta-2g)(1+\delta-g)}{(1-g)}. \tag{41}$$

Linearizing equation (41) in g under the assumption $g \ll 1$ leads to a simplified expression for δ_Q:

$$\delta_Q = \frac{Q_{33}-Q_{55}}{Q_{55}} 4g + \frac{Q_{33}-Q_{13}}{Q_{13}} 2(1+2\delta-2g). \tag{42}$$

Figure 5 shows an example of δ_Q as a function of δ and g. The parameters Q_{33} and Q_{55} are taken from the experimental results of Gautam et al. (2003) for Rim sandstone at a frequency of 25 Hz, while Q_{13} is assigned an arbitrary value. With this choice of Q components, the parameter δ_Q is quite sensitive to the squared velocity ratio g and reaches large negative values for hard rocks with $g > 0.35$. While the simplified equation (42) for δ_Q is sufficiently accurate for small magnitudes of both δ and g ($-0.1 < \delta < 0.2$ and $g < 0.2$), it produces a significant error for $g > 0.25$. In contrast to the velocity anisotropy parameter δ, the absolute value of δ_Q may be large (even greater than unity).

In combination with the Thomsen parameters for the velocity function, the parameters $1/Q_{33}$, $1/Q_{55}$, ϵ_Q, δ_Q, and γ_Q fully characterize the attenuation coefficients of P-, SV- and SH-waves. For isotropic velocity models with isotropic Q [equation (3)], equations (35) and (39) yield $\epsilon_Q = \delta_Q = 0$. If the medium is TI in terms of velocity but has isotropic Q, ϵ_Q still goes to zero, but δ_Q does not. Therefore, the attenuation coefficients of P- and SV-waves may be directionally dependent even in media with isotropic Q because of the coupling between the velocity and attenuation anisotropy.

5 APPROXIMATE ATTENUATION COEFFICIENTS FOR P- AND SV-WAVES

The exact equations for the P- and SV-wave attenuation coefficients are too complicated to be represented as explicit functions of the anisotropic parameters introduced above. It is possible, however, to obtain relatively simple approximations for the coefficient $\mathcal{A}$ by assuming simultaneously

1) weak attenuation ($\frac{1}{Q_{ij}} \ll 1$);

2) weak attenuation anisotropy ($|\epsilon_Q| \ll 1$, $|\delta_Q| \ll 1$); and

3) weak velocity anisotropy ($|\epsilon| \ll 1$, $|\delta| \ll 1$).

5.1 Approximate P-wave attenuation

To obtain the approximate P-wave attenuation coefficient as a function of phase angle, we express c_{ij} through the Thomsen parameters and Q_{ij} through the parameters ϵ_Q and δ_Q. Dropping terms quadratic in the anisotropy parameters ϵ, δ, ϵ_Q, and δ_Q in equation (28) yields

$$\mathcal{A}_P = \frac{1}{2Q_{33}}(1 + \delta_Q \sin^2\theta\cos^2\theta + \epsilon_Q \sin^4\theta). \tag{43}$$

In the linearized approximation, the angle dependence of $\mathcal{A}_P$ is governed by just the attenuation-anisotropy parameters ϵ_Q and δ_Q. The parameter δ_Q is responsible for the attenuation coefficient in near-vertical directions, while ϵ_Q controls $\mathcal{A}_P$ near the horizontal plane. If both ϵ_Q and δ_Q go to zero, the approximate coefficient $\mathcal{A}_P$ becomes isotropic.

It is interesting that equation (43) has the same form as the well-known Thomsen's (1986) weak-anisotropy approximation for P-wave phase velocity:

$$V_P = V_{P0}(1 + \delta \sin^2\theta\cos^2\theta + \epsilon \sin^4\theta). \tag{44}$$

To obtain equation (43) from the phase-velocity equation (44), we need to make the following substitutions: $V_{P0} \to \frac{1}{2Q_{33}}$, $\epsilon \to \epsilon_Q$, and $\delta \to \delta_Q$.

5.2 Approximate SV-wave attenuation

The linearized SV-wave attenuation coefficient has the form

$$\mathcal{A}_{SV} = \frac{1}{2Q_{55}} \frac{1 + \left(\frac{1-g}{g_Q}\sigma + \frac{1-g}{g}\sigma_Q\right)\sin^2\theta\cos^2\theta}{1 + \sigma\sin^2\theta\cos^2\theta}, \tag{45}$$

where g is defined in equation (40),

$$g_Q \equiv \frac{Q_{33}}{Q_{55}}, \tag{46}$$

and

$$\sigma \equiv \frac{V_{P0}^2}{V_{S0}^2}(\epsilon - \delta) = \frac{\epsilon - \delta}{g}. \tag{47}$$

If $|\sigma| \ll 1$, equation (45) can be further simplified to

$$\mathcal{A}_{SV} = \frac{1}{2Q_{55}}\left(1 + \sigma_Q \sin^2\theta \cos^2\theta\right), \tag{48}$$

where

$$\sigma_Q \equiv \frac{(1-g-g_Q)(\epsilon-\delta) + (1-g)(\epsilon_Q - \delta_Q)}{g g_Q}, \tag{49}$$

σ_Q determines the curvature of the SV-wave attenuation coefficient $\mathcal{A}_{SV}$ in the symmetry direction. According to equation (48), the attenuation for SV-waves becomes isotropic when

$$\epsilon_Q - \delta_Q = \left(\frac{g_Q}{1-g} - 1\right)(\epsilon - \delta). \tag{50}$$

Note that the assumption $|\sigma| \ll 1$ may not be valid for many TI formations because σ typically has a substantial magnitude even when $|\epsilon - \delta|$ is small.

5.3 Numerical examples

The accuracy of the approximate solutions (43) and (48) is illustrated by numerical tests in Figures 6–8. The P-wave attenuation coefficient in Figure 6 has an extremum (a maximum) near 43° because ϵ_Q and δ_Q have different signs. Otherwise, $\mathcal{A}_P$ varies monotonically between the vertical and horizontal directions. Approximation (48) predicts a minimum of the SV-wave attenuation coefficient at $\theta = 45°$. The curve of $\mathcal{A}_{SV}$ has a concave shape because σ_Q in equation (48) is negative and large by absolute value. The extrema of the exact attenuation coefficients in Figure 6 (solid lines) are shifted toward the vertical axis with respect to their approximate positions.

The approximations for both attenuation coefficients give satisfactory results for near-vertical propagation directions with angles θ up to about 30°. The error becomes noticeable for intermediate angles $30° < \theta < 75°$ and then decreases again near the horizontal plane. Note that both the velocity and attenuation anisotropy for the model from Figure 6 is not weak (see Figure 7), and the values of $\sigma = 0.75$ and $\sigma_Q = -2.13$ are particularly large.

Figure 8 displays the attenuation coefficients for a TI medium with $\epsilon_Q = \delta_Q = 0$. In agreement with equation (43), the P-wave attenuation is almost isotropic, and $\mathcal{A}_P$ traces out a curve close to a circle. The attenuation coefficient of SV-waves, however, deviates

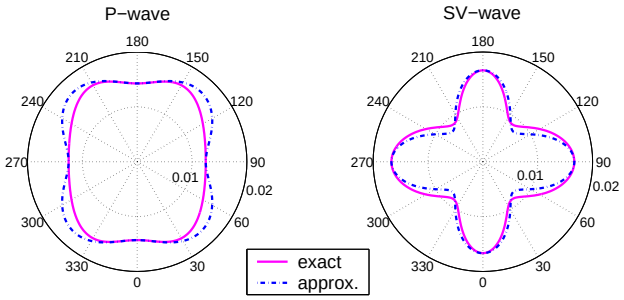

Figure 6. Attenuation coefficients of P-waves (left) and SV-waves (right) as functions of the phase angle. The solid curves are the exact values of $\mathcal{A}$ obtained by jointly solving equations (B3) and (B4); the dashed curves are the approximate coefficients from equations (43) and (48). The model parameters are V_{P0}=2.42 km/s, V_{S0}=1.4 km/s, $\epsilon = 0.4$, $\delta = 0.15$, $Q_{33} = 35$, $Q_{55} = 30$, $\epsilon_Q = -0.125$, and $\delta_Q = 0.94$.

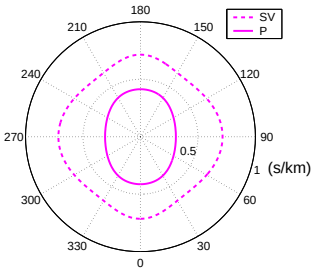

Figure 7. Slownesses of P- and SV-waves for the model from Figure 6.

from a circle because of the contribution of the velocity anisotropy in equation (48). Hence, isotropic Q in anisotropic media results in angle-dependent attenuation except for the special case of $Q_{ij} \equiv Q$.

If ϵ_Q and δ_Q satisfy condition (50), the attenuation coefficient of SV-waves is independent of direction (Figure 9). The curve of the P-wave coefficient $\mathcal{A}_P$ looks almost elliptical, but "elliptical attenuation anisotropy" for P-waves requires that $\epsilon_Q = \delta_Q$.

6 RADIATION PATTERNS IN ATTENUATIVE TI MEDIA

Here, we discuss the influence of attenuation on the radiation patterns of body waves excited by a point force in a homogeneous anisotropic medium. To obtain the Green's function, we apply the stationary-phase method to the Weyl-type integral for point-source radiation following the analytic results of Tsvankin and Chesnokov (1990).

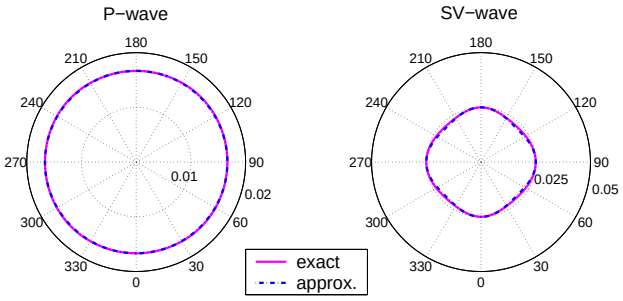

Figure 8. Attenuation coefficients of P-waves (left) and SV-waves (right) for $\epsilon_Q = \delta_Q = 0$. The solid curves are the exact values of $\mathcal{A}$ obtained by jointly solving equations (B3) and (B4); the dashed curves are the approximate coefficients from equations (43) and (48). The other model parameters are the same as those in Figure 6.

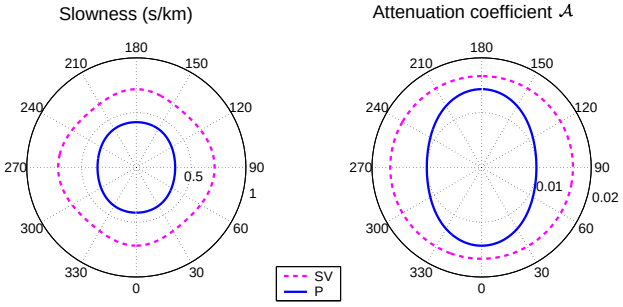

Figure 9. Slownesses (left) and the attenuation coefficients $\mathcal{A}$ (right) of P-waves (solid curves) and SV-waves (dashed) for a medium with isotropic SV-wave attenuation. The model parameters are V_{P0}=2.42 km/s, V_{S0}=1.4 km/s, $\epsilon = 0.18$, $\delta = 0.05$, $Q_{33} = 35$, $Q_{55} = 30$, $\epsilon_Q = -0.30$, and $\delta_Q = -0.40$ [δ_Q is calculated from equation (50)].

6.1 Radiation patterns for $Q_{ij} \equiv Q$

For the special case of attenuative media with $Q_{ij} \equiv Q$, the far-field spectrum of the body-wave radiation patterns given in Tsvankin and Chesnokov (1990) is multiplied with the factor (see Appendix D1)

$$\beta_Q = (1 - i\mathcal{A})^2 \exp\left(-\mathcal{A}\,\frac{\omega R}{V_G^\nu}\right), \tag{51}$$

where ω is the angular frequency, R is the distance between the source and receiver, V_G^ν is the group velocity, and ν denotes the wave type (i.e., P-, SV-, or SH-waves). In the limit of weak attenuation, $\mathcal{A} = 1/(2Q)$ and the factor β_Q becomes

$$\beta_Q \approx \exp\left(-\frac{\omega R}{2QV_G^\nu}\right). \tag{52}$$

Equation (51) shows that $Q_{ij} \equiv Q$ results in a purely isotropic attenuation even in general anisotropic media. However, this is not always true for the general isotropic matrix $\mathbf{Q}$ [equation (2)] that has two independent elements, Q_{33} and Q_{55}. Except for the special case of $Q_{ij} \equiv Q$, the attenuation coefficient and β_Q are always influenced by the velocity anisotropy.

6.2 Radiation patterns for TI Q

If the medium is transversely isotropic with respect to the velocity function and the matrix $\mathbf{Q}$ has TI symmetry, the far-field spectrum of the radiation patterns is multiplied with the factor in a form similar to that in expression (51) (see Appendix D2):

$$\beta_Q^\nu = (1 - i\mathcal{A}^\nu)^2 \exp\left[-\mathcal{A}^\nu\,\frac{\omega(r\sin\theta + z\cos\theta)}{V^\nu}\right]. \tag{53}$$

Note that $r\sin\theta + z\cos\theta = R\cos(\psi - \theta)$ and $V^\nu = V_G^\nu\cos(\psi - \theta)$ where θ is the phase angle corresponding to the stationary point (i.e., the angle between the wavefront normal and the vertical), ψ is the group (ray) angle corresponding to the source-receiver line. We then obtain

$$\beta_Q^\nu = (1 - i\mathcal{A}^\nu)^2 \exp\left(-\mathcal{A}^\nu\,\frac{\omega R}{V_G^\nu}\right). \tag{54}$$

The parameter $\mathcal{A}^\nu$ is the plane-wave attenuation coefficient discussed in detail above. In equation (51), $\mathcal{A}^\nu$ has to be computed for the phase direction corresponding to the stationary point. In a homogeneous medium, the actual (group) attenuation should be computed for the distance between the source and receiver. By analyzing the attenuation term in the integral representation of radiation patterns (Appendix D2), we obtain the group attenuation as

$$k_G^I = k\mathcal{A}^\nu\cos(\psi - \theta) = k^I\cos(\psi - \theta), \tag{55}$$

which is similar to the relationship between phase and group velocities in anisotropic media, but the phase attenuation is multiplied (rather than divided, as is the case for the velocities) with $\cos(\psi - \theta)$.

Under the assumption of weak attenuation and weak velocity and attenuation anisotropy, the P-wave attenuation coefficient in TI media is given in equation (43). The group attenuation coefficient of P-waves then becomes

$$k_{G,P}^I = k\,\frac{1}{2Q_{33}}(1 + \delta_Q\sin^2\theta\cos^2\theta + \epsilon_Q\sin^4\theta)\cos(\psi - \theta), \tag{56}$$

where k is the real part of the wavenumber.

6.3 Numerical example

To illustrate the relationship between the group and phase attenuation, we model SH-wave propagation in TI media with TI Q using a finite-difference solution of the wave equation (Figures 10–12). The finite-difference

code was written in Matlab for 2D TI models following the algorithm described in Carcione (2001). We discretize the model into 240×240 grid points, with a grid spacing of 5 m in both the vertical and horizontal directions. The SH-wave was excited by a point source at the center of the model. The central frequency of the wavelet is 21 Hz, the time step is 1 ms.

The SH-wave displacement for a model with $Q_{55} = 5$ and $Q_{66} = 10$ ($\gamma_Q = -0.5$) is displayed in Figure 10. The influence of attenuation is particularly convenient to study for SH-waves, because in purely elastic TI media the amplitude along the elliptical SH-wavefront is constant (Tsvankin, 2001), as illustrated by Figure 11. Since the quality factor increases away from the symmetry axis, the largest attenuation in Figure 10 is observed in the vertical direction.

The modeling results can be used to estimate the attenuation coefficient for a range of group angles ψ ($\psi = 0°$, $30°$, $45°$, $60°$, and $90°$). The group attenuation coefficient k_G^I satisfies the equation

$$\frac{A_1}{A_0} = \exp(-k_G^I R)\,, \tag{57}$$

where A_1 and A_0 are the spectral amplitudes at the central frequency obtained for the attenuative and associated purely elastic models, respectively. Hence,

$$k_G^I = \ln\left(\frac{A_0}{A_1}\right)/R\,. \tag{58}$$

The coefficient k_G^I estimated using equation (58) as a function of the group angle is marked by crosses in Figure 12. To verify the relationship between the group and phase attenuation coefficients, we first compute the phase coefficient $k^I(\theta)$ (solid line) from equations (32) and (34). Then we calculate the group angle ψ from the phase angle θ and obtain the group coefficient $k_G^I(\psi)$ (dashed line) from equation (55). This analytic coefficient k_G^I is sufficiently close to the measured value, which corroborates the validity of equation (55).

The above results suggest that the attenuation-anisotropy parameter γ_Q can be estimated from the group attenuation coefficient k_G^I in the following way. After obtaining the anisotropy parameter γ using velocity or traveltime measurements, we can calculate the phase angles corresponding to the group angles at the receiver locations. The phase attenuation coefficient k^I is then computed from equation (55) for the available range of phase angles, and γ_Q can be found from equation (34).

Accurate measurements of attenuation from seismic data, however, are not easy to implement in practice. Even in the simple modeling example in Figure 12, the coefficient k_G^I at a group angle of 30° is found with a significant error because of the instability of attenuation estimates in the frequency domain.

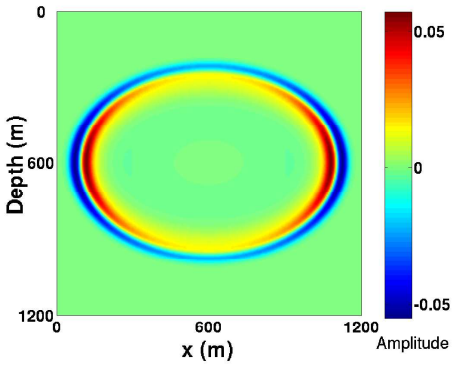

Figure 10. 2D snapshot of the SH-wavefront (particle displacement) propagating in a VTI medium with VTI Q. The model parameters are $V_{S0} = 1.83$ km/s, $\gamma = 0.44$, $Q_{55} = 5$, and $\gamma_Q = -0.5$; the time t=0.25 s.

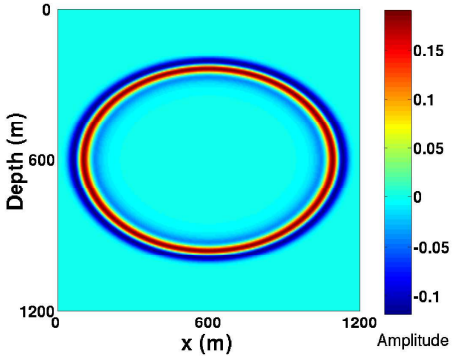

Figure 11. Same as Figure 10, but without attenuation ($Q_{55} = Q_{66} = \infty$).

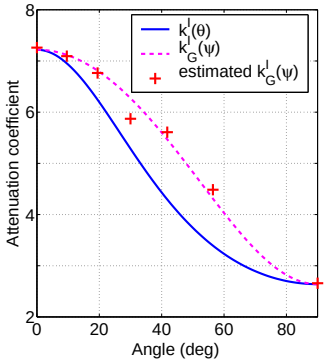

Figure 12. Comparison of the measured and computed group attenuation coefficients for the model from Figure 10. The solid curve is the phase attenuation coefficient k^I, the dashed curve is the group attenuation coefficient k_G^I computed from equation (55), and crosses are the values of k_G^I measured from the synthetic data using equation (58). The horizontal axis represents the phase angle for k^I and the group angle for k_G^I.

7 DISCUSSION AND CONCLUSIONS

The main goal of this paper is to build a practical analytic framework for describing amplitude distortions in attenuative transversely isotropic (TI) media. Although the symmetry axis was taken to be vertical, the results are valid for TI media with an arbitrary axis orientation. We assume that the wave propagation is *homogeneous* (i.e., the real and imaginary parts of the wave vector are parallel) and that the quality factor Q and phase velocity are independent of frequency for seismic bandwidth.

When attenuation is directionally dependent, the factor Q becomes a matrix with each component Q_{ij} defined as the ratio of the real and the imaginary parts of the corresponding stiffness coefficient. If the **Q**-matrix has a purely isotropic structure, it includes two independent elements responsible for the attenuation coefficients of P- and S-waves along the coordinate axes. For the special case $Q_{ij} \equiv Q$, plane-wave attenuation is independent of propagation direction, even for arbitrary velocity anisotropy. Analysis of point-source radiation for $Q_{ij} \equiv Q$ shows that the attenuation coefficient is constant along the wavefront, although the wavefront shape may be far from spherical.

Despite our insufficient understanding of the physical mechanism of attenuation, it seems likely that the attenuation anisotropy (defined by the structure of the matrix **Q**) has the same or higher symmetry as the velocity anisotropy. The main emphasis of this work is on TI velocity models with either TI or isotropic attenuation, and the symmetry axes for the velocity and attenuation anisotropy are assumed to be parallel.

Analysis of the Christoffel equation shows that the perturbation of the phase-velocity function caused by the attenuation is of the second order and can be ignored. To facilitate the description of TI attenuation, we introduce Thomsen-style parameters responsible for directionally dependent attenuation coefficients of P-, SV-, and SH-waves. The reference "isotropic" values are the P- and S-wave attenuation coefficients in the vertical (symmetry) direction. Following the idea of Thomsen notation for velocity anisotropy, we supplement the reference quantities with three dimensionless anisotropic parameters denoted by ϵ_Q, δ_Q, and γ_Q. The parameter ϵ_Q is equal to the fractional difference between the P-wave horizontal and vertical attenuation coefficients, and γ_Q denotes the same quantity for SH-waves. Similar to the Thomsen parameter δ for velocity anisotropy, the parameter δ_Q is designed to describe near-vertical variations in P-wave attenuation. Therefore, δ_Q is defined as a normalized second derivative of the P-wave attenuation coefficient at vertical incidence. In contrast to ϵ_Q and γ_Q, δ_Q depends on the Thomsen parameter δ and, therefore, reflects the coupling between the attenuation and velocity anisotropy.

While the attenuation coefficient of SH-waves represents a relatively simple function of the parameter γ_Q, exact equations for the attenuation anisotropy of P- and SV-waves are much more involved. The Thomsen-style parameters, however, can be used to obtain the linearized attenuation coefficients under the assumptions of weak attenuation and weak velocity and attenuation anisotropy. The approximate P-wave attenuation coefficient has the same form as the linearized phase-velocity function, with the vertical velocity V_{P0} replaced by $\frac{1}{2Q_{33}}$, ϵ by ϵ_Q, and δ by δ_Q. Although the approximate solution for the attenuation coefficient for SV-waves involves contributions of both attenuation and velocity parameters, it has the same angle dependence as its phase-velocity counterpart.

Numerical examples demonstrate that the approximate solutions adequately reproduce the character of attenuation anisotropy and are sufficiently accurate for moderately anisotropic (in terms of both velocity and attenuation) TI models. Computation of the exact attenuation coefficients also proves that the isotropic **Q**-matrix in TI media does not necessarily yield isotropic attenuation due to the influence of the velocity anisotropy.

The improved understanding of plane-wave propagation helps to describe the influence of attenuation anisotropy on point-source radiation. Application of the stationary-phase method to the Weyl integral for the wavefield from a point force allowed us to derive the far-field Green's function in attenuative media. In the limit of weak attenuation, the amplitude of each mode is multiplied with an exponential factor governed by the "group" attenuation coefficient that corresponds to the source-receiver direction. The relationship between the group and phase (plane-wave) attenuation coefficient is controlled by the difference between the group and phase angles that can be computed from the phase-velocity function. These results provide a basis for estimating the attenuation-anisotropy parameters from field data and correcting the AVO response for angle-dependent attenuation.

8 ACKNOWLEDGMENTS

We are grateful to Michael Batzle, Maarten de Hoop (both CSM) and members of the A(nisotropy)-Team of the Center for Wave Phenomena (CWP) at CSM for helpful discussions and to reviewers of the manuscript. The support for this work was provided by the Consortium Project on Seismic Inverse Methods for Complex Structures at CWP and by the Chemical Sciences, Geosciences and Biosciences Division, Office of Basic Energy Sciences, U.S. Department of Energy.

9 REFERENCES

Arts, R. J., and Rasolofosaon P. N. J., 1992, Approximation of velocity and attenuation in general

anisotropic rocks: 62nd Ann. Internat. Mtg., Soc Expl. Geophys., Expanded Abstracts, 640–643.

Blangy, J. P., 1994, AVO in transversely Isotropic media—An overview: Geophysics **49**, 775–781.

Carcione, J. M., 1997, Reflection and transmission of qP-qS plane waves at a plane boundary between viscoelastic transversely isotropic media: Geophys. J. Int. **129**, 669-680.

Carcione, J. M., 2000, A model for seismic velocity and attenuation in petroleum source rocks: Geophysics **65**, 1080–1092.

Carcione, J. M., 2001, Wave fields in real media: wave propagation in anisotropic, anelastic, and porous media: Pergamon.

Chichinina, T., Sabinin, V., and Ronquillo-Jarrillo, G., 2004, Azimuthal variation of P-wave attenuation for fracture characterization: Geophysics (submitted).

Gautam, K., Batzle, M., and Hofmann, R., 2003, Effect of fluids on attenuation of elastic waves: 73rd Ann. Internat. Mtg., Soc Expl. Geophys., Expanded Abstracts, 1592-1595.

Helbig, K., 1994, Foundations of anisotropy for exploration seismics: Pergamon.

Hosten, B., Deschamps, M., and Tittmann B. R., 1987, Inhomogeneous wave generation and propagation in lossy anisotropic solids: application to the characterization of viscoelastic composite materials: J. Acoust. Soc. Am., **82**, 1763–1770.

Johnston, D. H., and Toksöz, M. N., 1981, Definitions and terminology, *in* Seismic wave attenuation: Geophysics reprinted series, No. 2.

Lynn, H. B., Campagna, D., Simon, K. M., and Beckham, W. E., 1999, Relationship of P-wave seismic attributes, azimuthal anisotropy, and commercial gas pay in 3-D P-wave multiazimuth data, Rulison Field, Piceance Basin, Colorado: Geophysics, **64**, 1293–1311.

Prasad, M., and Nur, A., 2003, Velocity and attenuation anisotropy in reservoir rocks: 73rd Ann. Internat. Mtg., Soc Expl. Geophys., Expanded Abstracts, 1652-1655.

Rathore, J. S., Fjaer, E., Holt, R. M., and Renlie, L., 1995, Acoustic anisotropy of a synthetic sandstone with controlled crack geometry: Geophys. Prosp., **43**, 805–829.

Sayers, C. M., 1994, The elastic anisotropy of shales: J. Geophys. Res., **99**(B1), 767–774.

Thomsen , L., 1986, Weak elastic anisotropy: Geophysics, **51**, 1954–1966.

Tsvankin, I., and Chesnokov, E. M., 1990, Synthesis of body wave seismograms from point sources in anisotropic media: J. Geophys. Res., **95**(B7), 11317–11331.

Tsvankin, I., 1995, Seismic wavefields in layered isotropic media: Course Notes, Samizdat Press.

Tsvankin, I., 2001, Seismic signatures and analysis of reflection data in anisotropic media: Elsevier.

Ursin, B., and Stovas, A., 2002, Reflection and transmission responses of a layered isotropic viscoelastic medium: Geophysics, **67**, 307–323.

APPENDIX A: PLANE SH-WAVES IN ATTENUATIVE TI MEDIA

The Christoffel equation for a plane SH-wave propagating in an attenuative VTI medium yields

$$\tilde{c}_{66}\tilde{k}_1^2 + \tilde{c}_{55}\tilde{k}_3^2 - \rho\omega^2 = 0\,, \tag{A1}$$

where $\tilde{c}_{ij} = c_{ij} + ic_{ij}^I$ are the complex stiffness coefficients. The complex wavenumber is represented as $\tilde{k}_i = k_i - ik_i^I$, where $k^I = \sqrt{k_1^{I2} + k_2^{I2} + k_3^{I2}}$ is the attenuation coefficient. Hereafter, we limit the discussion to *homogeneous* wave propagation by assuming $\mathbf{k} \parallel \mathbf{k}^I$.

A1 VTI Q

For the general VTI form of the matrix $\mathbf{Q}$, equation (A1) becomes

$$[(c_{66} + ic_{66}^I)n_1^2 + (c_{55} + ic_{55}^I)n_3^2](k - ik^I)^2 - \rho\omega^2 = 0\,, \tag{A2}$$

which can be divided into the real part

$$(c_{66}n_1^2 + c_{55}n_3^2)[k^2 - (k^I)^2] + (c_{66}^I n_1^2 + c_{55}^I n_3^2)2kk^I - \rho\omega^2 = 0\,, \tag{A3}$$

and the imaginary part

$$(c_{66}^I n_1^2 + c_{55}^I n_3^2)[k^2 - (k^I)^2] - (c_{66}n_1^2 + c_{55}n_3^2)2kk^I = 0\,, \tag{A4}$$

where $n_1 = \sin\theta$ and $n_3 = \cos\theta$.

By expressing the complex stiffnesses through the Q_{ij} components and introducing $c_{66} = c_{55}(1+2\gamma)$, equation (A4) can be rewritten as

$$k^2 - (k^I)^2 - 2Q_{55}\alpha kk^I = 0\,, \tag{A5}$$

where

$$\alpha \equiv \frac{(1+2\gamma)n_1^2 + n_3^2}{(1+2\gamma)\dfrac{Q_{55}}{Q_{66}}n_1^2 + n_3^2}\,. \tag{A6}$$

The only physically meaningful solution k^I of equation (A5) is

$$k^I = k(\sqrt{1 + (Q_{55}\alpha)^2} - Q_{55}\alpha)\,. \tag{A7}$$

The real part, equation (A3), then reduces to

$$(c_{66}n_1^2 + c_{55}n_3^2)\left[k^2 - (k^I)^2 + \frac{2kk^I}{Q_{55}\alpha}\right] - \rho\omega^2 = 0\,, \tag{A8}$$

which gives the following expression for the phase velocity of the SH-wave:

$$V_{SH} = V_{SH}^{\text{elast}} \cdot \xi_Q\,; \tag{A9}$$

$V_{SH}^{\rm elast}$ is the SH-wave phase velocity in purely-elastic VTI media:

$$V_{SH}^{\rm elast} = \sqrt{\frac{c_{66}n_1^2 + c_{55}n_3^2}{\rho}}, \tag{A10}$$

ξ_Q is the factor responsible for the influence of the anisotropic attenuation on the phase velocity:

$$\xi_Q = \sqrt{\frac{2(\sqrt{1+(Q_{55}\alpha)^2} - Q_{55}\alpha)(1+(Q_{55}\alpha)^2)}{Q_{55}\alpha}}. \tag{A11}$$

For weak attenuation, $\xi_Q \approx 1 + \frac{1}{2(Q_{55}\alpha)^2}$.

A2 Isotropic Q

Isotropic Q for the SH-wave propagation implies $Q_{55} = Q_{66}$. The imaginary part of equation (A1) then reduces to

$$k^2 - (k^I)^2 - 2Qkk^I = 0, \tag{A12}$$

and $\alpha = 1$. Hence, for isotropic Q we have

$$k^I = k(\sqrt{1+Q^2} - Q) \tag{A13}$$

and

$$\xi_Q = \sqrt{\frac{2(\sqrt{1+Q^2} - Q)(1+Q^2)}{Q}}. \tag{A14}$$

APPENDIX B: PLANE P- AND SV-WAVES IN ATTENUATIVE TI MEDIA

For P- and SV-waves, the Christoffel equation gives the following equation for the the complex wavenumbers:

$$\begin{aligned}&(\tilde{c}_{11}\tilde{k}_1^2 + \tilde{c}_{55}\tilde{k}_3^2 - \rho\omega^2)(\tilde{c}_{55}\tilde{k}_1^2 + \tilde{c}_{33}\tilde{k}_3^2 - \rho\omega^2)\\ &-[(\tilde{c}_{13}+\tilde{c}_{55})\tilde{k}_1\tilde{k}_3]^2 = 0.\end{aligned} \tag{B1}$$

B1 VTI Q

When the matrix $\mathbf{Q}$ has VTI symmetry, equation (B1) yields

$$\begin{aligned}&\{[(c_{11}+ic_{11}^I)n_1^2 + (c_{55}+ic_{55}^I)n_3^2](k - ik^I)^2 - \rho\omega^2\}\cdot\\ &\{[(c_{55}+ic_{55}^I)n_1^2 + (c_{33}+ic_{33}^I)n_3^2](k - ik^I)^2 - \rho\omega^2\}\\ &\{[(c_{13}+c_{55}) + i(c_{13}^I + c_{55}^I)]n_1n_3kk^I\}^2 = 0.\end{aligned} \tag{B2}$$

The real and the imaginary parts are given, respectively, by

$$\begin{aligned}&[(c_{11}n_1^2 + c_{55}n_3^2)\mathcal{K}_1^a - \rho\omega^2][(c_{55}n_1^2 + c_{33}n_3^2)\mathcal{K}_1^b - \rho\omega^2]\\ &-(c_{13}+c_{55})^2n_1^2n_3^2\mathcal{K}_1^{c2} = 0,\end{aligned} \tag{B3}$$

and

$$\begin{aligned}&(c_{11}n_1^2 + c_{55}n_3^2)\mathcal{K}_2^a[(c_{55}n_1^2 + c_{33}n_3^2)\mathcal{K}_1^b - \rho\omega^2] +\\ &(c_{55}n_1^2 + c_{33}n_3^2)\mathcal{K}_2^b[(c_{11}n_1^2 + c_{55}n_3^2)\mathcal{K}_1^a - \rho\omega^2]\\ &-(c_{13}+c_{55})^2n_1^2n_3^2\mathcal{K}_1^c\mathcal{K}_2^c = 0,\end{aligned} \tag{B4}$$

where

$$\begin{aligned}&\mathcal{K}_1^a = \mathcal{K}_1 + \frac{\Delta^a}{Q_{33}}2kk^I,\ \mathcal{K}_2^a = \mathcal{K}_2 - \frac{\Delta^a}{Q_{33}}[k^2 - (k^I)^2],\\ &\mathcal{K}_1^b = \mathcal{K}_1 + \frac{\Delta^b}{Q_{33}}2kk^I,\ \mathcal{K}_2^b = \mathcal{K}_2 - \frac{\Delta^b}{Q_{33}}[k^2 - (k^I)^2],\\ &\mathcal{K}_1^c = \mathcal{K}_1 + \frac{\Delta^c}{Q_{33}}2kk^I,\ \mathcal{K}_2^c = \mathcal{K}_2 - \frac{\Delta^c}{Q_{33}}[k^2 - (k^I)^2],\end{aligned} \tag{B5}$$

$$\mathcal{K}_1 = k^2 - (k^I)^2 + \frac{2kk^I}{Q_{33}}, \tag{B6}$$

$$\mathcal{K}_2 = \frac{1}{Q_{33}}[k^2 - (k^I)^2] - 2kk^I, \tag{B7}$$

and

$$\begin{aligned}\Delta^a &= \frac{c_{11}n_1^2}{c_{11}n_1^2 + c_{55}n_3^2}\frac{Q_{33}-Q_{11}}{Q_{11}} +\\ &\quad\frac{c_{55}n_3^2}{c_{11}n_1^2 + c_{55}n_3^2}\frac{Q_{33}-Q_{55}}{Q_{55}},\\ \Delta^b &= \frac{c_{55}n_1^2}{c_{55}n_1^2 + c_{33}n_3^2}\frac{Q_{33}-Q_{55}}{Q_{55}},\\ \Delta^c &= \frac{c_{13}}{c_{13}+c_{55}}\frac{Q_{33}-Q_{13}}{Q_{13}} + \frac{c_{55}}{c_{13}+c_{55}}\frac{Q_{33}-Q_{55}}{Q_{55}}.\end{aligned} \tag{B8}$$

Using equation (B4), we find

$$\mathcal{K}_2 = -\frac{A\Delta^a + B\Delta^b - C\Delta^c}{A+B-C}\frac{[k^2 - (k^I)^2]}{Q_{33}}, \tag{B9}$$

where

$$\begin{aligned}A &= (c_{11}n_1^2 + c_{55}n_3^2)[(c_{55}n_1^2 + c_{33}n_3^2)\mathcal{K}_1^b - \rho\omega^2],\\ B &= (c_{55}n_1^2 + c_{33}n_3^2)[(c_{11}n_1^2 + c_{55}n_3^2)\mathcal{K}_1^a - \rho\omega^2],\\ C &= 2(c_{13}+c_{55})^2n_1^2n_3^2\mathcal{K}_1^c.\end{aligned} \tag{B10}$$

Equation (B9) can be simplified by assuming weak attenuation and weak attenuation anisotropy (see Appendix C).

B2 Special case: $Q_{ij} \equiv Q$

Consider the special case of identical Q components, $\frac{c_{11}}{c_{11}^I} = \frac{c_{33}}{c_{33}^I} = \frac{c_{13}}{c_{13}^I} = \frac{c_{55}}{c_{55}^I} = Q$. Equation (B1) becomes

$$\begin{aligned}&\left[(c_{11}n_1^2 + c_{55}n_3^2)\mathcal{K}_1 - \rho\omega^2 + i(c_{11}n_1^2 + c_{55}n_3^2)\mathcal{K}_2\right]\cdot\\ &\left[(c_{55}n_1^2 + c_{33}n_3^2)\mathcal{K}_1 - \rho\omega^2 + i(c_{55}n_1^2 + c_{33}n_3^2)\mathcal{K}_2\right]\\ &-[(c_{13}+c_{55})n_1n_3(\mathcal{K}_1 + i\mathcal{K}_2)]^2 = 0,\end{aligned} \tag{B11}$$

where $\mathcal{K}_1$ and $\mathcal{K}_2$ are defined in equations (15) and (10).

The only physically meaningful solution of the imaginary part of equation (B11) is $\mathcal{K}_2 = 0$, which then yields the same expression of k^I as that in equation (A13).

Solving the real part of equation (B11), we obtain the phase velocities in the form

$$V_{\{P,SV\}} = V_{\{P,SV\}}^{\rm elast}\cdot\xi_Q, \tag{B12}$$

where ξ_Q is given in equation (A14), and $V^{\rm elast}_{\{P,SV\}}$ is P- or SV-wave phase velocity in the reference purely-elastic VTI medium:

$$V^{\rm elast}_{\{P,SV\}} = \frac{1}{2\rho}\cdot\Big\{(c_{11}+c_{55})n_1^2+(c_{33}+c_{55})n_3^2 \pm \sqrt{[(c_{11}-c_{55})n_1^2-(c_{33}-c_{55})n_3^2]^2+4(c_{13}+c_{55})^2n_1^2n_3^2}\Big\}^{\frac{1}{2}}. \tag{B13}$$

APPENDIX C: APPROXIMATE SOLUTIONS FOR WEAK ATTENUATION AND WEAK ATTENUATION ANISOTROPY

C1 Attenuation coefficient for P- and SV-waves

Here, we simplify the attenuation coefficient derived in Appendix B1 under the assumption of weak attenuation and weak attenuation anisotropy. If the attenuation is weak ($k^I \ll k$), the term $(k^I)^2$ in the difference $k^2-(k^I)^2$ can be ignored. If the attenuation anisotropy is weak, then $|\frac{Q_{33}-Q_{11}}{Q_{11}}| \ll 1$, $|\frac{Q_{33}-Q_{55}}{Q_{55}}| \ll 1$, and $|\frac{Q_{33}-Q_{13}}{Q_{13}}| \ll 1$. The terms $\frac{\Delta^a}{Q_{33}}2kk^I$, $\frac{\Delta^b}{Q_{33}}2kk^I$, and $\frac{\Delta^c}{Q_{33}}2kk^I$ in equations (B5) are of the second-order compared to k^2, and $\mathcal{K}_1^a \approx \mathcal{K}_1^b \approx \mathcal{K}_1^c \approx \mathcal{K}_1$. It can be further shown that for weak attenuation $\mathcal{K}_1 \approx k^2$, which allows us to represent equations (B10) as

$$\begin{aligned} A &= (c_{11}n_1^2+c_{55}n_3^2)[(c_{55}n_1^2+c_{33}n_3^2)k^2-\rho\omega^2],\\ B &= (c_{55}n_1^2+c_{33}n_3^2)[(c_{11}n_1^2+c_{55}n_3^2)k^2-\rho\omega^2],\\ C &= 2(c_{13}+c_{55})^2n_1^2n_3^2k^2. \end{aligned} \tag{C1}$$

In the limit of weak attenuation, equation (B9) takes the form

$$k^2-(k^I)^2-2Q_{33}kk^I = -\frac{A\Delta^a+B\Delta^b-C\Delta^c}{A+B-C}k^2, \tag{C2}$$

and

$$\mathcal{A} = \frac{k^I}{k} = \sqrt{1+Q_{33}^2+\mathcal{H}}-Q_{33}, \tag{C3}$$

where

$$\mathcal{H} = \frac{A\Delta^a+B\Delta^b-C\Delta^c}{A+B-C}. \tag{C4}$$

Further linearization of equation (C3) yields

$$\mathcal{A} = \frac{1}{2Q_{33}}(1+\mathcal{H}). \tag{C5}$$

C2 Parameter δ_Q

The attenuation-anisotropy parameter δ_Q is defined through the second derivative of $\mathcal{A}_P$ with respect to the phase angle θ at vertical incidence:

$$\left.\frac{d^2\mathcal{A}_P}{d\theta^2}\right|_{\theta=0} = 2\,\mathcal{A}_P|_{\theta=0}\,\delta_Q. \tag{C6}$$

Substitution of $\mathcal{A}$ from equation (C5) leads to the following expression for δ_Q:

$$\delta_Q = \frac{1}{2}\left.\frac{d^2\mathcal{H}}{d\theta^2}\right|_{\theta=0} \tag{C7}$$

for the case of weak attenuation. By evaluating $\left.\frac{d^2\mathcal{H}}{d\theta^2}\right|_{\theta=0}$ and taking into account that for P-waves $\mathcal{H}|_{\theta=0}=0$ and $\left.\frac{\partial\mathcal{H}}{\partial\theta}\right|_{\theta=0}=0$, we obtain

$$\delta_Q = \frac{\frac{Q_{33}-Q_{55}}{Q_{55}}c_{55}\frac{(C_{13}+c_{33})^2}{(c_{33}-c_{55})}+2\frac{Q_{33}-Q_{13}}{Q_{13}}c_{13}(c_{13}+c_{55})}{c_{33}(c_{33}-c_{55})}. \tag{C8}$$

APPENDIX D: POINT-SOURCE RADIATION IN ANISOTROPIC ATTENUATIVE MEDIA

The derivation in this section follows the methodology discussed by Tsvankin and Chesnokov (1990) and Tsvankin (1995) for purely elastic media. The wavefield from a point force (i.e., the Green's function) is decomposed into plane waves by applying Fourier transforms to the wave equation and then performing integration over one of the wavenumbers. The zero-order approximation of the stationary phase method (SPM) is used to evaluate the resulting integral and obtain the displacement in the far field.

D1 Models with $Q_{ij} \equiv Q$

The wave equation for a point force embedded in an arbitrarily anisotropic, attenuative, homogeneous medium can be written as

$$\rho\frac{\partial^2 u_i}{\partial t^2} - \tilde{c}_{ijkl}\frac{\partial^2 u_k}{\partial x_j\partial x_l} = h_i(t)\delta(\mathbf{x}), \tag{D1}$$

where ρ is the density, $\mathbf{u}(t,\mathbf{x})$ is the displacement vector, $h_i(t)$ is the source signal, and $\delta(\mathbf{x})$ is the 3D δ function that indicates that the source is located at the origin of the Cartesian coordinate system. $\tilde{c}_{ijkl}$ is the fourth-rank tensor of the complex stiffnesses, $\tilde{c}_{ijkl} = c_{ijkl} + ic^I_{ijkl}$.

By representing the displacement vector through a 3D Fourier integral, Tsvankin and Chesnokov (1990) obtained a decomposition of point-source radiation into plane waves that can be adapted for attenuative media. We consider an arbitrarily anisotropic medium with $\frac{c_{ij}}{c^I_{ij}} \equiv Q$ for any $i,j = 1 \sim 6$ and assume homogeneous

wave propagation ($\mathbf{k} \parallel \mathbf{k^I}$). (The tensor c_{ijkl} is replaced here with the stiffness matrix c_{ij} using Voigt notation.) Then the spectrum $\tilde{\mathbf{S}}(\omega, \mathbf{x})$ of the displacement $\tilde{\mathbf{u}}(t, \mathbf{x})$ is given by

$$\tilde{\mathbf{S}}^{\nu}(\omega, \mathbf{x}) = 2\pi i\omega \sum_{\nu=1}^{3} \int_{-\infty}^{\infty} \int_{-\infty}^{\infty} \tilde{\mathbf{U}}^{\nu}(\omega, p_1, p_2) \tilde{f}_Q^3 \exp\left[-i\omega(p_1 x_1 + p_2 x2 + p_3 x_3)\tilde{f}_Q\right] dp_1 dp_2 , \quad \text{(D2)}$$

where $\tilde{\mathbf{p}} = \dfrac{\tilde{\mathbf{k}}}{\omega}$ is the complex slowness vector, $\tilde{\mathbf{U}}^{\nu}(\omega, p_1, p_2) = \mathrm{Res}[\dfrac{1}{\tilde{D}(p_3)} \tilde{\mathbf{G}}^{\mathrm{ad}} \mathbf{F}(\omega)]_{p_3^{\nu}}$, $\tilde{\mathbf{G}}^{\mathrm{ad}}$ is the complex matrix adjoint to $\tilde{\mathbf{G}}$, $\tilde{D}(p_3) = \det\tilde{\mathbf{G}}$, p_3^{ν} is the root of $\tilde{D}(p_3) = 0$, ν denotes the wave type (P, S_1, or S_2), and $F_i(\omega) = \int_{-\infty}^{+\infty} h_i(t) \exp(-i\omega t) dt$. In the limit of weak attenuation, $\tilde{f}_Q = 1 - i(\sqrt{1+Q^2} - Q)$ for the special case $Q_{ij} \equiv Q$.

We introduce the cylindrical coordinate system ($p_1 = p_0 \cos\phi$, $p_2 = p_0 \sin\phi$) and rewrite equation (D2) in the form

$$\tilde{\mathbf{S}}^{\nu}(\omega, \mathbf{x}) = 2\pi i\omega \sum_{\nu=1}^{3} \int_0^{\infty} \int_0^{2\pi} \tilde{\mathbf{U}}^{\nu}(\omega, p_0, \phi) \tilde{f}_Q^3 \cdot \exp\left[-i\omega[p_0 r \cos(\phi - \alpha) + p_3^{\nu} z]\tilde{f}_Q\right] p_0 dp_0 d\phi . \quad \text{(D3)}$$

The phase of the exponential term in equation (D3) can be represented as

$$\Phi(p_0, \phi) = c^{\nu} z + g^{\nu} \cos[B^{\nu} - (\phi - \alpha)]\tilde{f}_Q , \quad \text{(D4)}$$

where $g^{\nu} = \sqrt{(p_0 r + d^{\nu} z)^2 + (e^{\nu} z)^2}$, $\sin B^{\nu} = \dfrac{e^{\nu} z}{g^{\nu}}$, and $\cos B^{\nu} = \dfrac{p_0 r + d^{\nu} z}{g^{\nu}}$. Because of the influence of the attenuation, the phase term $\Phi(p_0, \phi)$ is multiplied with the complex factor $\tilde{f}_Q$. For the special case $Q_{ij} \equiv Q$, $\tilde{f}_Q$ is independent of the slowness components and, as discussed below, does not change the stationary point obtained by the SPM.

Following the approach of Tsvankin and Chesnokov (1990), we represent the azimuthal dependence of $\tilde{U}_i^{\nu}$ and the vertical slowness component p_3^{ν} by several terms of the Fourier series expansion:

$$\tilde{U}_i^{\nu}(p_0, \phi) = \sum_{m=-l}^{l} \tilde{A}_{i,n}^{\nu}(p_0) \exp\left[im(\phi - \alpha)\right] , \quad \text{(D5)}$$

$$p_3^{\nu}(p_0, \phi) = c^{\nu}(p_0) + d^{\nu}(p_0)\cos(\phi - \alpha) + e^{\nu}(p_0)\sin(\phi - \alpha) . \quad \text{(D6)}$$

Evaluation of the integral over azimuth in equation (D3) yields

$$\tilde{S}_i^{\nu}(\omega, \mathbf{x}) = 4\pi^2 i\omega \tilde{f}_Q^3 \int_0^{\infty} \int_0^{2\pi} \exp\left(-i\omega \tilde{f}_Q c^{\nu} z\right) \sum_{m=-l}^{l} \frac{J_m(\omega \tilde{f}_Q g^{\nu})}{i^n} \tilde{A}_n^{i\nu}(p_0) \exp(imB^{\nu}) p_0 dp_0 . \quad \text{(D7)}$$

Application of the zero-order approximation of the stationary phase method gives the same stationary point, $\phi_0^{\nu} = \alpha + B^{\nu}$, as the one for purely elastic media. Using an asymptotic representation of the Bessel function $J_m(x)$ for large values of the argument x, we find the spectrum of the displacement in the far field:

$$\tilde{S}_i^{\nu}(\omega, \mathbf{x}) = \frac{i\tilde{f}_Q^2}{\omega V^{\nu}} \tilde{U}_i^{\nu} \exp\left[-i\frac{\omega \tilde{f}_Q}{V^{\nu}}(r\sin\theta + z\cos\theta)\right] \cdot \left. \frac{\sin\theta(\dfrac{\cos\theta}{V^{\nu}} + \dfrac{\partial p^{\nu}}{\partial\theta}\sin\theta)}{\sqrt{(\dfrac{\sin\theta}{V^{\nu}} r + d^{\nu} z)\dfrac{\partial^2 \Phi_1}{\partial\theta^2}}} \right|_{\theta = \theta_0^{\nu}} , \quad \text{(D8)}$$

where

$$\frac{\partial^2 \Phi_1}{\partial\theta^2} = (r\sin\theta + z\cos\theta)(\frac{1}{V^{\nu}} - \frac{\partial^2 p^{\nu}}{\partial\theta^2}) + \frac{2}{V^{\nu}} \frac{(r\cos\theta - z\sin\theta)^2}{r\sin\theta + z\cos\theta} . \quad \text{(D9)}$$

Substitution of $\tilde{f}_Q = 1 - i(\sqrt{1+Q^2} - Q)$ into equation (D8) leads to

$$\tilde{S}_i^{\nu}(\omega, \mathbf{x}) = [1 - i(\sqrt{1+Q^2} - Q)]^2 \exp\left[-\frac{\omega}{V^{\nu}}(\sqrt{1+Q^2} - Q)(r\sin\theta + z\cos\theta)\right] \tilde{S}_i^{\nu,\mathrm{elast}}(\omega, \mathbf{x}) , \quad \text{(D10)}$$

where $\tilde{S}_i^{\nu,\mathrm{elast}}(\omega, \mathbf{x})$ is the result for purely elastic media in equation (20) of Tsvankin and Chesnokov (1990). Introducing the attenuation coefficient $\mathcal{A} = \sqrt{1+Q^2} - Q$, in equation (D10), we obtain

$$\tilde{S}_i^{\nu}(\omega, \mathbf{x}) = (1 - i\mathcal{A})^2 \exp\left[-\frac{\omega(r\sin\theta + z\cos\theta)}{V^{\nu}}\mathcal{A}\right] \times \tilde{S}_i^{\nu,\mathrm{elast}}(\omega, \mathbf{x}) . \quad \text{(D11)}$$

Note that $r\sin\theta + z\cos\theta = R\cos(\psi - \theta)$ and $V^{\nu} = V_G^{\nu}\cos(\psi - \theta)$, where R is the distance between the source and receiver, ψ is the group angle, and V_G^{ν} is the group velocity. We then obtain

$$\tilde{S}_i^{\nu}(\omega, \mathbf{x}) = (1 - i\mathcal{A})^2 \exp\left(-\mathcal{A}\frac{\omega R}{V_G^{\nu}}\right) \tilde{S}_i^{\nu,\mathrm{elast}}(\omega, \mathbf{x}) . \quad \text{(D12)}$$

D2 Models with VTI Q

For anisotropic media with VTI Q, the exponential term in the integral representation (D8) of $\tilde{S}_i(\omega, \mathbf{x})$ still has the form $\exp\left[-i\dfrac{\omega \tilde{f}_Q^{\nu}}{V^{\nu}}(r\sin\theta + z\cos\theta)\right]$, where, for weak attenuation, $\tilde{f}_Q^{\nu} = 1 - i\mathcal{A}^{\nu}$; $\mathcal{A}^{\nu}$ is the attenuation coefficient for the wave type ν. For VTI media with VTI

Q, approximate expression for $\mathcal{A}^\nu$ are given in equation (43) for P-waves and (45) for SV-waves. The phase term of $\tilde{S}_i(\omega, \mathbf{x})$ from equation (D8) has the form

$$\Phi = -\frac{1}{V^\nu}(r\sin\theta + z\sin\theta)\,. \tag{D13}$$

Applying the stationary-phase condition $\dfrac{d\Phi}{d\theta} = 0$, we arrive at the following equation for the stationary-phase point θ:

$$\tan\theta = \frac{r}{z} + \frac{1}{z\cos\theta}V^\nu\frac{\partial p^\nu}{\partial\theta}(r\sin\theta + z\cos\theta)\,. \tag{D14}$$

Substitution of the stationary-phase angle θ from equation (D14) into the attenuation term $\exp\left[-i\dfrac{\omega\mathcal{A}^\nu}{V^\nu}(r\sin\theta + z\cos\theta)\right]$ yields the "group" attenuation in the source-receiver direction:

$$k_G^I = \frac{\omega}{V^\nu}\mathcal{A}^\nu\frac{r\sin\theta + z\cos\theta}{\sqrt{r^2+z^2}}\,, \tag{D15}$$

and

$$k_G^I = k^I\cos(\psi - \theta)\,, \tag{D16}$$

where ψ is the group angle.

The far-field spectrum $\tilde{S}_i(\omega, \mathbf{x})$ then becomes

$$\tilde{S}_i^\nu(\omega, \mathbf{x}) = (1 - i\mathcal{A}^\nu)^2\exp\left[-\frac{\omega(r\sin\theta + z\cos\theta)}{V^\nu}\mathcal{A}^\nu\right] \times\tilde{S}_i^{\nu,\text{elast}}(\omega, \mathbf{x})\,. \tag{D17}$$